Received: 26 October 2023 | Revised: 5 March 2024 | Accepted: 2 April 2024

DOI: 10.1002/jbm.b.35405

RESEARCH ARTICLE

Improving material properties of a poloxamer P407 hydrogel-based hydroxyapatite bone substitute material by adding silica—A comparative in vivo study

Peer W. Kämmerer[1,2] | Diana Heimes[1] | Franziska Zaage[3] | Cornelia Ganz[3] | Bernhard Frerich[2] | Thomas Gerber[3] | Michael Dau[2]

[1]Department of Oral, Maxillofacial Plastic Surgery, University Medical Center Mainz, Mainz, Germany

[2]Department of Oral, Maxillofacial Plastic Surgery, University Medical Center Rostock, Rostock, Germany

[3]Institute of Physics, Rostock University, Rostock, Germany

Correspondence
Diana Heimes, Department of Oral, Maxillofacial Plastic Surgery, University Medical Center Mainz, 55131 Mainz, Germany.
Email: diana.heimes@icloud.com; diana.heimes@unimedizin-mainz.de

Abstract

The structure and handling properties of a P407 hydrogel-based bone substitute material (BSM) might be affected by different poloxamer P407 and silicon dioxide (SiO_2) concentrations. The study aimed to compare the mechanical properties and biological parameters (bone remodeling, BSM degradation) of a hydroxyapatite: silica (HA)-based BSM with various P407 hydrogels in vitro and in an in vivo rat model. Rheological analyses for mechanical properties were performed on one BSM with an SiO_2-enriched hydrogel (SPH25) as well on two BSMs with unaltered hydrogels in different gel concentrations (PH25 and PH30). Furthermore, the solubility of all BSMs were tested. In addition, 30 male Wistar rats underwent surgical creation of a well-defined bone defect in the tibia. Defects were filled randomly with PH30 ($n = 15$) or SPH25 ($n = 15$). Animals were sacrificed after 12 ($n = 5$ each), 21 ($n = 5$ each), and 63 days ($n = 5$ each). Histological evaluation and histomorphometrical quantification of new bone formation (NB;%), residual BSM (rBSM;%), and soft tissue (ST;%) was conducted. Rheological tests showed an increased viscosity and lower solubility of SPH when compared with the other hydrogels. Histomorphometric analyses in cancellous bone showed a decrease of ST in PH30 ($p = .003$) and an increase of NB (PH30: $p = .001$; SPH: $p = .014$) over time. A comparison of both BSMs revealed no significant differences. The addition of SiO_2 to a P407 hydrogel-based hydroxyapatite BSM improves its mechanical stability (viscosity, solubility) while showing similar in vivo healing properties compared to PH30. Additionally, the SiO_2-enrichment allows a reduction of poloxamer ratio in the hydrogel without impairing the material properties.

KEYWORDS
bone substitute, hydrogel, low crystalline hydroxyapatite, poloxamer 407 (P407), rat animal model, silicon dioxide

1 | INTRODUCTION

Bone defects may occur in different regions of the human skeleton due to trauma, surgery, inflammation, cancer, or even physiological bone loss. Defects that will not heal spontaneously despite surgical stabilization and require further intervention are defined as critical-size defects. While the use of autologous bone grafts—based on their osteoconductive, osteoinductive, and osteogenic properties—is still the first choice for augmentation of critical-size bone defects, the clinical use of those grafts is limited by donor-site morbidity and the amount of available material.[1–3] Accordingly, bone substitute materials (BSMs) may be an appropriate alternative to support bone regrowth.[4] Even so, no BSM meets all requirements for bone regeneration as obtained with autologous bone.[5]

Besides biocompatibility and promoting bone regeneration, good handling properties of BSM are important factors for clinical success. Most BSM is provided in granular form, but—from a clinical point of view—this application form is rather disadvantageous. Granular BSM is not easy to apply and contour into desired shapes. While a strong condensation of the granular BSM during application might slow down the degradation and, therefore, the bone remodeling, a loosened BSM can increase neovascularization and bone remodeling.[6] An approach for improving the respective handling properties might be using additional carrier materials.

The combination of BSM and bioactive components became increasingly popular. Those molecules, drugs, and cells that can activate intracellular and extracellular signaling pathways enhance tissue healing, promote osteogenesis, and accelerate regeneration.[7] Hyaluronic acid, for example, is a linear polyanionic glycosaminoglycan and a main component of the human body's extracellular matrix.[8] Studies have shown that it enhances osteogenesis, promotes bone regeneration,[9] and enables even distribution and a higher density of the newly regenerated bone.[8] In preclinical studies, hyaluronic acid has been shown to promote the osteoconductive potential of synthetic and xenogeneic bone substitutes.[10,11] Only a few prospective clinical studies examine the effect of hyaluronic acid on maxillofacial bone regeneration.[12,13] Even if the results of case series, preclinical, and in vitro studies are promising, clinical studies still lack evidence for a significant effect.

Therefore, a combined product consisting of a BSM, and a carrier material would be desirable. Attempts have been made to generate fixed combinations to enhance handling properties and bone formation.[10]

Poloxamers are copolymers with amphiphilic properties consisting of a central hydrophobic block of polypropylene oxide flanked by two hydrophilic blocks of polyethylene oxide. Poloxamer can form micelles in water or other solvents.[14,15] With increasing polymer concentration, the micelles can self-assemble and form a gel structure for embedding compact substances like drugs.[16] The American Food and Drug Administration listed Poloxamer 407 (P407) to be an inactive and pharmaceutical excipient.[17] P407 is nontoxic and biocompatible when in contact with vital tissue such as cells and body fluids.[18] In an animal experiment, P407, combined with hydroxyapatite- and biphasic calcium phosphate-based BSM, showed similar bone healing effects compared to the BSM without P407.[19]

The major inorganic component of natural bone is hydroxyapatite, which contains elements such as magnesium, silicon, and other metal ions.[20] Based on the assumed function of silicon in bone formation,[21–24] combinations of P407 with silicon dioxide (SiO_2) nanoparticles might be a promising approach to increase BSM function further. In tissue engineering, silicates are preferred over phosphate due to their superior physicochemical and biological properties. Silicon has been reported to stimulate osteogenic differentiation by releasing silicate-containing ionic products and enhancing bone regeneration.[25] But while the effects of a SiO_2-enriched hydroxyapatite BSM on bone remodeling are well researched,[24,26,27] it is unknown if there is any biologically relevant effect of SiO_2 in a poloxamer gel serving as an admixture of a hydroxyapatite BSM. SiO_2 binds polymer chains—like in P407—on the silica surface[28] and forms micelles.[29]

The primary aim of this study was to test the mechanical properties of various poloxamer P407 hydrogel-based hydroxyapatite BSMs by rheological measurements and solubility analyses. Following the results from material characterization, the second part of the study at hand focused on the comparison of the two BSMs (PH30 vs. SPH25) regarding new bone formation and degradation in an in vivo animal rat model.

2 | MATERIALS AND METHODS

2.1 | Study materials

The basis for the tested BSMs was a synthetic non-sintered low crystalline hydroxyapatite material (NanoBone® S39, Artoss GmbH, Rostock, Germany) embedded in a highly porous silica matrix (ratio 61:39 wt %). The bone substitute granule is comprised of hydroxyapatite (HA) crystallites with platelet dimensions of 3-nm thickness, 30-nm width, and 50-nm length ensconced within a silica gel matrix with an interconnection nanopore structure.[30] Its synthesis is achieved through a sol–gel method executed at temperatures not exceeding 700°C, thereby circumventing the sintering of low crystalline hydroxyapatite.[31] The biomaterial is distinguished by numerous accessible bonds, yielding an internal surface area of up to 84 m^2g^{-1}. The pore size distribution within the silica gel matrix ranges from 10 to 20 nm in diameter. Macroscopically, the granules exhibit a conical morphology akin to fir cones, possessing an average length and diameter of 2 mm and 0.6 mm, respectively, coupled with a porosity within the range of 60%–80%.[32]

This material was combined with a poloxamer P407 hydrogel (Kolliphor® P407, Sigma Aldrich, St. Louis, Missouri, USA) in three compositions. While two hydrogels were composed of poloxamer P407 at different concentrations (PH25: 25 wt % poloxamer P407; PH30: 30 wt % poloxamer P407), the third hydrogel (SPH25) comprised poloxamer P407 and weakly crosslinked silica nanoaggregates in an aqueous solution.

The resulting and studied BSM groups (Table 1) were as follows:

1. Hydroxyapatite: silica mixture with 25 wt % P407 hydrogel (PH25).
2. Hydroxyapatite: silica mixture with 30 wt % P407 hydrogel (PH30).
3. Hydroxyapatite: silica mixture with 25 wt % P407 hydrogel containing 3 wt % SiO_2 (SPH25).

Even as all used hydroxyapatite mixture contained silica, only SPH25 has silica in the P407 hydrogel.

After manufacture, all materials were sterilized by gamma irradiation via a $Cobalt^{60}$ source (Synergy Health Radeberg GmbH, Applied Sterilization Technologies, Radeberg, Germany) at a 25–40 kGy dose rate.

2.2 | Rheological studies

Rheological analyses were performed using an oscillation rheometer (ARES, T. A. Instruments, New Castle, USA) with cone-plate geometry. Viscosities of PH25, PH30, and SPH25 were described as a function of the shear rate at a constant frequency: 1 Hz frequency and in the range of shear rates between 0.1 and 1000 s^{-1}. The sample volume measurements (about 2.5 mL) were conducted at 22°C, respectively 37°C. All tests were made in triplicate.

Based on the results of the conducted rheological analyses, further analyses focused on PH30 and SPH25 only.

2.3 | Solubility tests

The adhesive properties of PH30 and SPH25 were measured in a solubility test with simulated body fluid (SBF) to describe the resistance of the carrier material in typical SBF-influenced defects. Each 1.00 g synthetic non-sintered low crystalline hydroxyapatite material (HA) and 0.05 g of the respective hydrogels were incubated in 7-mL SBF at 37°C. Over 90 min, the mass of the remaining coherent parts was measured at seven different points (after 1, 10, 15, 30, 45, 60, and 90 min). All values were expressed as relative mass (each time) to starting mass (baseline). All tests were made in triplicate.

TABLE 1 Composition of tested bone substitute materials.

Group	Granular bone substitute material	Hydrogel
PH25	synthetic unsintered nanocrystalline hydroxyapatite material: porous silica matrix (ratio 61:39 wt %).	poloxamer P407: water (ratio 25:75 wt %)
PH30	synthetic unsintered nanocrystalline hydroxyapatite material: porous silica matrix (ratio 61:39 wt %)	poloxamer P407: water (ratio 30:70 wt %)
SPH25	synthetic unsintered nanocrystalline hydroxyapatite material: porous silica matrix (ratio 61:39 wt %)	poloxamer P407: silica:water (ratio 25:3:72 wt %)

Note: Group allocation with respective composition of tested composite bone substitute material.
Abbreviation: wt %, weight percent.

2.4 | Animal model and procedures

The present study used an established animal rat tibia model.[26] The experiment was approved by the State Office of Agriculture, Food Safety and Fishery Mecklenburg-Vorpommern, Germany (LVL M-V/TSD/7221.3-1.1-101/11) and followed the National Institutes of Health guidelines for the care and use of laboratory animals as well the ARRIVE Guidelines for Reporting Animal Research.[33]

Thirty male adult Wistar rats (average mean body weight: 465 ± 33 g) were included in the study. The animals were kept in a room with a 12/12 h dark–light cycle with food and water ad libitum. After the operation, the animals were kept separate in type III cages, and enrichment was provided by paper roll and rodent wood.

All performed surgical interventions were conducted under general anesthesia with an intraperitoneally injected mixture of 40-mg ketamine hydrochloride (Ketamin® 10%, Belapharm, Vercha, Germany) and 3.5 mg xylazine hydrochloride (Rompun® 2%, Bayer HealthCare Animal Health, Leverkusen, Germany) per 400 mg animal bodyweight. Following anesthesia, the median aspect of the tibia was exposed via longitudinal incisions. One predefined 3.5 mm diameter mono-cortical and medullar defect was created on the proximal area of the tibia in each animal ($n = 15$) (Figure 1) using a dental drill bur F3004 (Meisinger, Neuss, Germany). The cavities were randomly

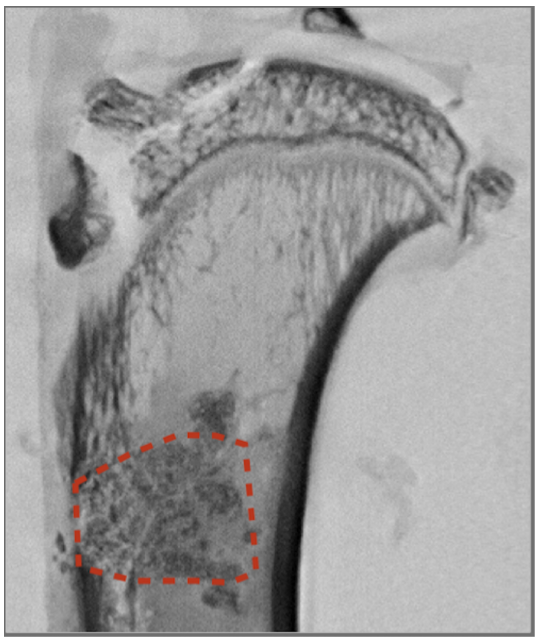

FIGURE 1 Micro CT scan of the proximal tibia defect filled with bone substitute material.

(achieved using a computer-generated list) filled with PH30 respectively SPH25. After closing the periosteum, muscle, and skin in layers using absorbable suture material (Vicryl®, Ethicon, Norderstedt, Germany), the animals received intramuscular analgesia via 0.5 mg carprofen (Rimadyl®, Zoetis Germany GmbH, Berlin, Germany). Metamizole (Novaminsulfon-ratiopharm®, ratio-pharm GmbH, Ulm, Germany) was also applied to the drinking water postoperatively for the first 5 days.

The animals were sacrificed after 12, 21, and 63 days ($n = 5$ each per time point) by an intraperitoneal injection of 55-mg pentobarbital hydrochloride (Narcoren®, Merial GmbH, Hallbergmoos, Germany) per 1000 mg of animal bodyweight and the tibiae were harvested for the further histological examination. The bones were fixed in 4% phosphate-buffered formalin for 7 days and decalcified in 20% EDTA (pH 7.2–7.4) over 2 weeks. Decalcified specimens were embedded in paraffin, and 3-µm sections were cut and stained with hematoxylin–eosin (HE) and Goldner's trichrome staining for standard histological analysis.

2.5 | Histomorphometric qualitative analysis

All histological analyses were performed in HE staining using a Zeiss light microscope (Axio Imager.M2 microscope, Zeiss, Oberkochen, Germany). All histological figures were captured with a microscope camera (AxioCam MRc5 camera, Zeiss, Oberkochen, Germany) that was connected to an automatic scanning table (M-686K011, Wienecke & Sinske GmbH, Gleichen, Germany). Additional analyses were made in Goldner's trichrome staining.

The analysis focused on visualizing the integration and degradation of the bone substitute material, the bone formation, and the remodeling process by measuring newly formed bone (NB), soft tissue (ST), and residual graft at different time points. The qualitative histological evaluation included observation of multinuclear cells, osteoblasts, and blood vessels participating in biomaterial integration and degradation.

2.6 | Histomorphometric quantitative analysis

For a standardized analysis, regions of interest were predefined as described before.[26] The total defect area was separated into a cancellous (CD) and a medullary defect area (MD; Figure 2). The primary defect lines in the cortical bone were defined as lateral borders of the CD. In contrast, primary defect lines in the cancellous, MD were defined as lateral borders of the respective area. Double the width of the cancellous bone height set the inner border of the MD. The combination of both areas described the total defect area (TD). To determine values for the NB, residual bone substitute material (rBSM), and ST, the areas were marked and measured as pixels using Adobe Photoshop CS6 (Adobe Systems Inc., San Jose, CA). The pixel number of each marked area (NB, rBSM, respectively ST) was set in relation to the pixel number of the selected area (cancellous defect area, medullary defect area, and total defect area) and expressed as a percentage rate (%).

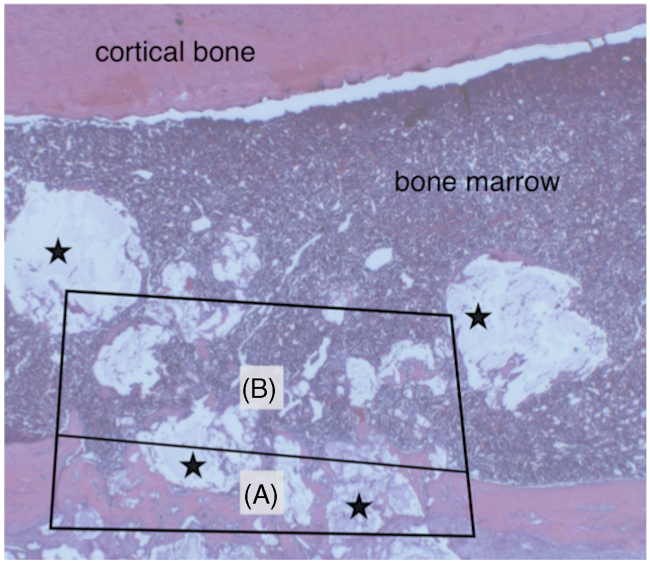

FIGURE 2 Defined areas of interest; total defect area separated into cancellous defect area (A) and medullary defect area (B); magnification ×5[26]; ★ biomaterial.

2.7 | Statistics

Statistics were performed using the software package SPSS version 20.0 (SPSS Inc., Chicago, IL, USA). All results in the presented study were expressed as arithmetic means ± standard error of the mean (SEM) and rounded to one decimal digit. Before testing for statistical significance, all variables were evaluated for normal distribution by applying the Shapiro–Wilk test. Two-way analysis of variance for BSM (first way) and time (second way) followed by subsequent repeated measures within one group and analyses between the groups at each time point were made by using an ANOVA (parametric data) respectively a Kruskal–Wallis rank sum test (nonparametric data). Depending on the presence or absence of normal distribution, the Student's *T* and Mann–Whitney tests for continuous variables were used for pairwise comparison at each time point. Because of multiple testing for comparison of histological calculations (NB, soft tissue, and rBSM), Bonferroni corrections were applied. The *p*-values of ≤.0166 were accepted as significant. Bar and line charts with error bars (SEM) were used for data illustration.

3 | RESULTS

3.1 | Rheological measurements and solubility testing

In contrast to values found at 37°C, viscosity at 22°C was decreased in all groups (PH25, PH30, and SPH25), and the shear rates were increased. Additionally, the increased poloxamer concentration in the pure poloxamer hydrogel (PH25 vs. PH30) was associated with increased viscosity. Adding silica particles (3 wt %) to the lower-dosed poloxamer hydrogel (SPH25) also increased viscosity. These effects were observed at 22°C (Figure 3A) and 37°C (Figure 3B).

Solubility of PH30 and SPH25 at SBF at 37°C showed similar values at 1 min. Still, at later points (starting at 10 min), a lower solubility of SPH25 compared with PH30 was observed (Figure 4).

3.2 | In vivo experiments

For all animals, postoperative healing was uneventful, and no postoperative complications were observed. In total, 30 samples at the three different time points (12, 21, and 63 days) were evaluated ($n = 5$ each).

3.3 | Histomorphometric qualitative analysis

Light microscopic analyzes showed that both tested bone grafts were well tolerated. Osteoblasts, multinuclear cells, new blood vessels, and new bone formation were observed in both groups. After 12 days, osteoblasts and multinuclear cells were found on the surface of the bone graft granules in PH30 and SPH25 (Figure 5). Additionally, bone formation, blood vessels, and ST were detected in both groups (Figure 5). The defect area remained visible in PH30 and SPH25 63 days after implantation. Residues of bone graft substitute material (rBSM) were found even after 63 days in both groups (PH30 and SPH25; Figure 6).

Optical microscopy analyses could not detect the P407-based hydrogel at any time, neither in PH30 nor SPH25. Analyzes of Goldner's trichrome staining revealed no additional information.

3.4 | Histomorphometric quantitative analysis

In total, an increase in the NB and a decrease in rBSM was observed within the CD in both groups over time (Table 2). A similar decrease of rBSM was also detected in the MD in PH30 and SPH25 (Table 2). In contrast to these results, the amount of NB remained unchanged in both BSM over time. Histomorphometric analyses regarding NB, rBSM, and ST in sections of TD did not reveal any further information.

3.5 | 12 days

A slightly nonsignificant higher amount of NB (PH30: 20.6 ± 4.5% vs. SPH25: 31.2 ± 2.6%; $p = .078$) and nonsignificant lower values of rBSM (PH30: 38.1 ± 3.5% vs. SPH25: 23.9 ± 5.4%; $p = .058$) were detected for SPH25 in the CD. Analyses in MD regarding NB, rBSM, and ST showed no differences between PH30 and SPH25 ($p > .4$ each) (Table 2).

3.6 | 21 days

After 21 days, a nonsignificant increase of NB and a decrease in rBSM in the CD was observed in PH30 and SPH25 compared with values at

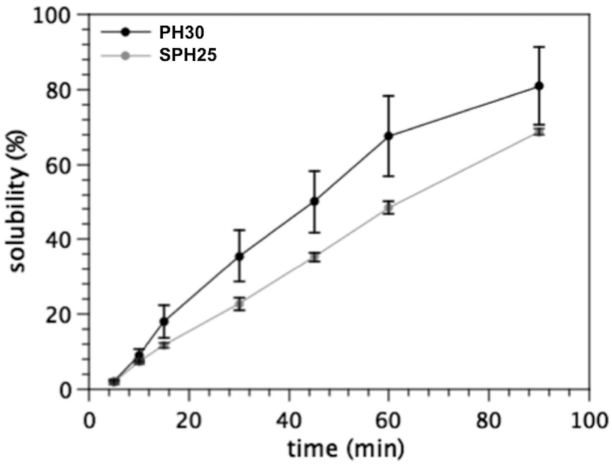

FIGURE 4 Line charts of solubility for PH30 and SPH25 in simulated body fluid at 37°C.

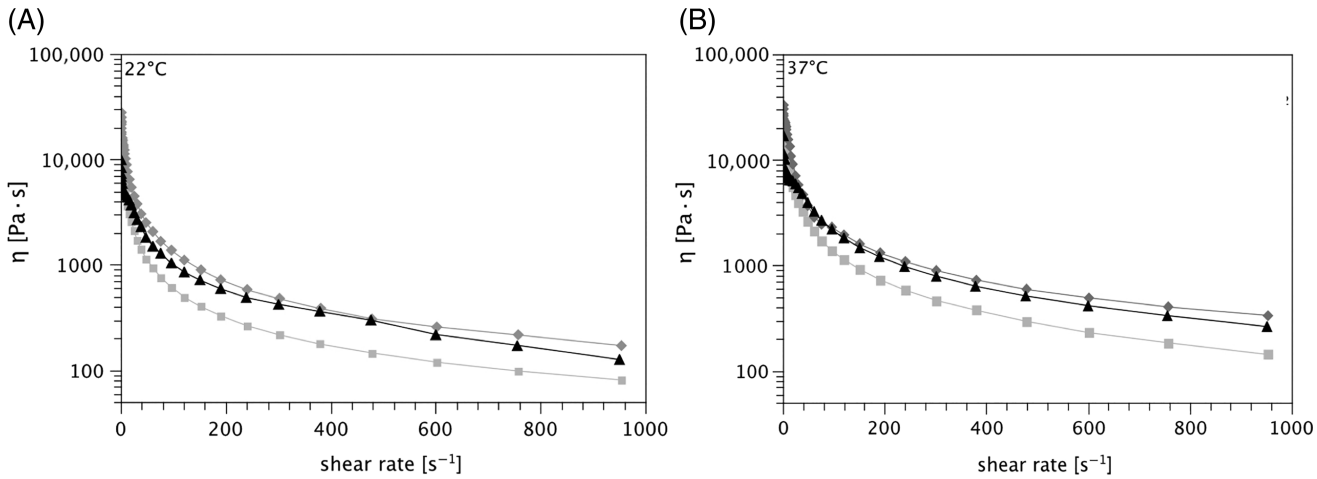

FIGURE 3 Line chart of poloxamer P407 hydrogel viscosity at 22°C (A) and 37°C (B) as a function of shear rate; PH25 (■) and PH30 (▲) in comparison to SPH25 (◆).

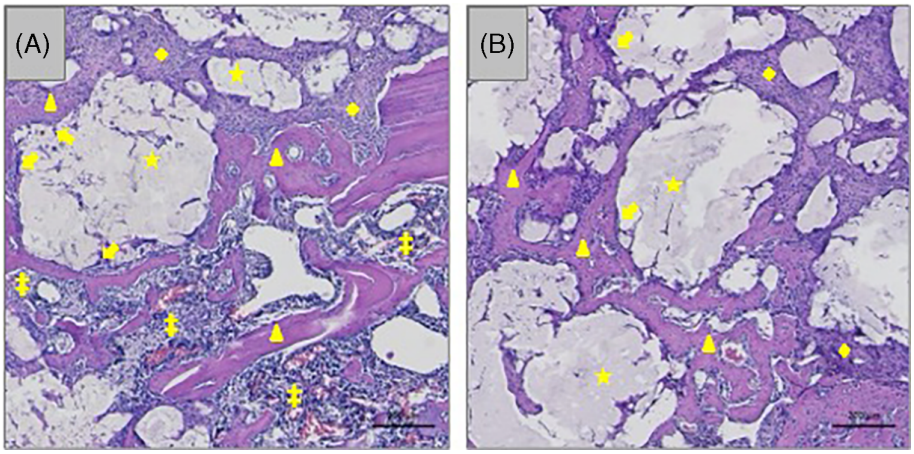

FIGURE 5 Histological figure at 12 days postoperatively. (A) residual bone substitute material and newly-formed bone in SPH25 (HE staining); (B) residual bone substitute material and newly-formed bone in PH30 (HE staining); scale bars: 200 µm. ★ biomaterial; ▲ newly formed bone; ➞ multinuclear cells; + blood vessel; ◆ soft tissue; and ‡ bone marrow.

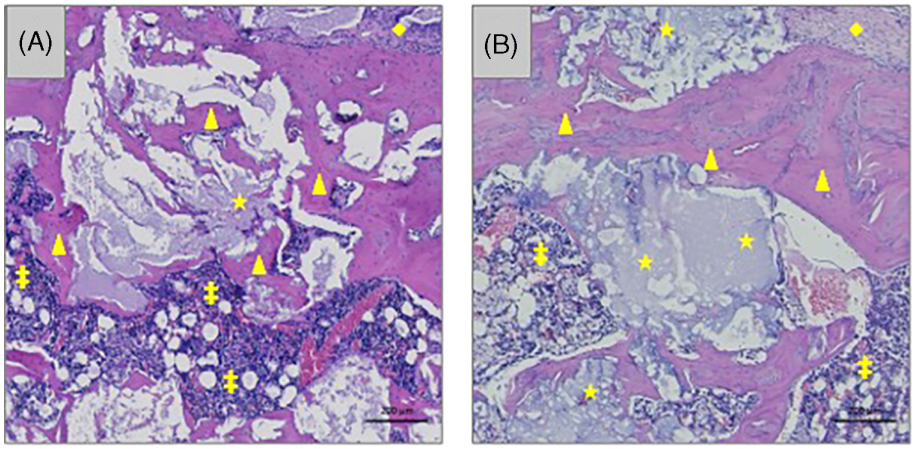

FIGURE 6 Histological figure at 63 days postoperatively. (A) residual bone substitute material and newly-formed bone in PH30 (HE staining); (B) residual bone substitute material and newly-formed bone in SPH25 (HE staining); scale bars: 200 µm. ★ biomaterial; ▲ newly formed bone; ◆ soft tissue; and ‡ bone marrow.

TABLE 2 Histomorphometrical quantitative analyses after 12, 21, and 63 days in PH30 versus SPH25 (mean ± SEM).

	Cancellous defect area (CD)			Medullary defect area (MD)		
	PH30	SPH25	*p*-value	PH30	SPH25	*p*-value
12 days	$n = 5$	$n = 5$		$n = 5$	$n = 5$	
Residual BSM (%)	38.1 (±3.5)	23.9 (±5.4)	.058 ◆	38.9 (±3.5)	33.7 (±8.1)	.578 ◆
Soft tissue (%)	41.2 (±3.8)	44.9 (±3.3)	.488 ◆	39.1 (±2.9)	45.2 (±6.7)	.436 ◆
Newly-formed bone (%)	20.6 (±4.5)	31.2 (±2.6)	.078 ◆	22.0 (±3.1)	21.1 (±1.9)	.811 ◆
21 days	$n = 5$	$n = 5$		$n = 5$	$n = 5$	
Residual BSM (%)	25.2 (±5.5)	19.1 (±4.8)	.432 ◆	37.5 (±3.6)	27.6 (±1.1)	.050 ◆
Soft tissue (%)	40.1 (±6.9)	42.6 (±6.2)	.799 ◆	44.0 (±5.1)	54.6 (±3.0)	.110 ◆
Newly-formed bone (%)	34.7 (±5.8)	38.3 (±4.7)	.643 ◆	18.4 (±2.4)	17.7 (±2.5)	.844 ◆
63 days	$n = 5$	$n = 5$		$n = 5$	$n = 5$	
Residual BSM (%)	25.9 (±4.5)	13.3 (±4.4)	.081 ◆	27.9 (±3.8)	26.4 (±4.2)	.805 ◆
Soft tissue (%)	15.0 (±5.1)	26.7 (±8.5)	.076 ▲	48.8 (±6.4)	51.2 (±2.9)	.602 ▲
Newly-formed bone (%)	59.1 (±5.2)	60.0 (±8.8)	.936 ◆	23.3 (±3.8)	22.3 (±2.0)	.823 ◆

Note: Histomorphometrical measurement after 12, 21, and 63 days for PH25 versus SPH25 (mean ± standard error of the mean); ◆ Student's *T* test respectively ▲ Mann–Whitney test; accepted significant level with Bonferoni-correction $p < .0166$.

Abbreviations: BSM, bone substitute material; PH30, hydroxyapatite bone substitute material with 30 wt % poloxamer P407 hydrogel; SPH, hydroxyapatite bone substitute material with SiO_2-enriched 25 wt % P407 hydrogel.

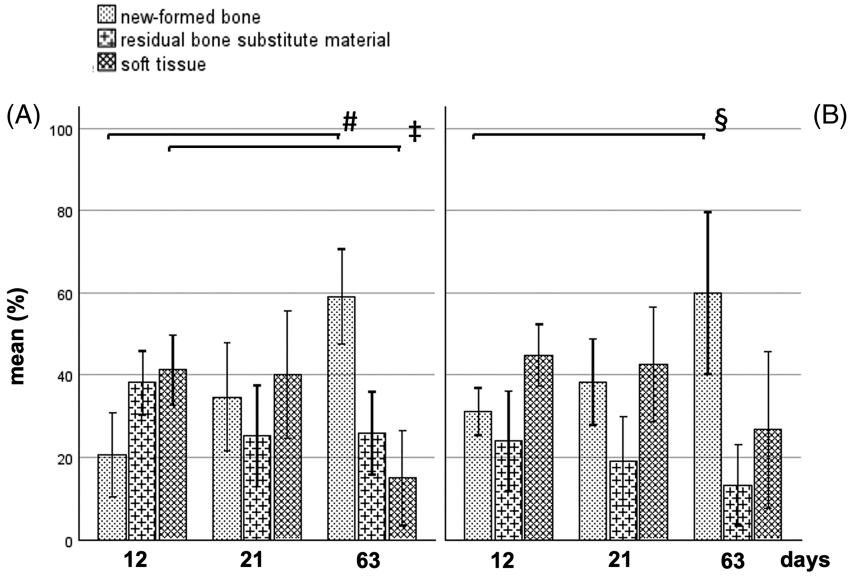

FIGURE 7 Bar charts of histomorphometry analyses regarding newly formed bone, residual bone substitute material, soft tissue in cancellous defect area over time. (A) mean values of newly-formed bone, residual bone substitute material, soft tissue (%) in PH30 over different points in time; (B) mean values of newly-formed bone, residual bone substitute material, soft tissue (%) in SPH25 over different points in time; # $p < .001$, § $p = .014$, and ‡ $p = .003$.

day 12. In contrast to changes in CD, the observed values of NB, rBSM, and ST for PH30 and SPH25 in MD stayed stable over time. Comparing measured values at 21 days one by one between the groups showed no differences regarding the amount of NB, ST, and rBSM ($p > .05$ each) (Table 2).

3.7 | 63 days

While the values of rBSM, ST, and NB in CD showed a strong change over time for both groups (Figure 7), the amount of NB in MD remained stable (Table 2). Generally, higher values of NB (PH30: $p = .001$; SPH25: $p = .003$) and ST (PH: $p = .003$; SPH25: $p = .076$) were detected in CD compared with MD values. While rBSM in PH30 had similar values in CD and MD, the rBSM in SPH25 in CD was about 0.5-fold the value in MD ($p = .003$). The direct comparison of PH30 and SPH25 for each parameter (NB, ST, and rBSM) showed no differences between the tested BSMs in the respective defect areas.

4 | DISCUSSION

The study aimed to examine a poloxamer P407 hydrogel-based hydroxyapatite bone substitute with the addition of SiO_2 regarding its in vitro and in vivo characteristics and handling properties. The SiO_2-enriched hydrogel (SPH25) improved its mechanical stability through an increased viscosity and a lower solubility when compared with the hydrogels without adding silica. Besides, similar biological properties of the tested BSMs—SPH25 (SiO_2-enriched) and PH25/PH30 (non-SiO_2-enriched)—were detected in vivo.

Previous studies have shown that non-sintered BSM exhibits an increased formation of new bone compared with sintered BSM.[34] This might be explained by the higher percentage of pores facilitating the ingrowth of new bone and blood vessels.[35,36] The BSM used in the present study is known to have a chiseled-ruffled, large surface with a mean pore size distribution of 330–530 µm representing the optimal pore size for osteoconduction.[35,37] The material has further been supposed to activate platelets, to store and release platelet-derived cytokines,[38] and therefore combine the advantages of a slow degradable material and the regenerative action of human blood. In a rabbit model, Dau et al. found faster resorption kinetics of non-sintered BSM, which was accelerated polymer. The group explained this effect by decreasing compression forces, allowing faster degradation.[34]

SiO_2 is an integral part of natural bone. It can also promote osteogenic differentiation by recruiting bone marrow stem cells in the early stage of healing and mineralization in the midterm phase; it furthermore improves the adhesion and proliferation of osteoblasts.[20,39,40] A combination of β-tricalcium phosphate with silicon has been shown to exhibit enhanced bioactivity and promote osteogenesis by modulating type I collagen production and osteocalcin. The amount of SiO_2 has even been correlated with an immunomodulating effect—the silicate ions may promote the macrophage transition and inhibit the expression of M1 biomarkers in the early phase of inflammation, which would suggest a positive effect on neovascularization by promoting macrophage polarization into the M2 phenotype and an anti-inflammatory effect via the secretion of IL-10.[39]

While SiO_2 is important in bone development, repair,[21] and increasing the metabolic activity and proliferation of osteoblasts,[41,42] little is known about the effect of SiO_2 on P407 hydrogel. Based on the missing detection of the P407 hydrogel material (PH respectively SPH) after 12 days and later, complete degradation of the used P407 hydrogels might be imaginable. This theory is supported by other studies lacking the ability to detect any poloxamer after 4 weeks in an in vivo rabbit model.[34] On the other hand, the P407 hydrogel might be dissolved by the histological processing of the sample before the histomorphometry analysis. Contrarily to the observed nondetection of the P407 hydrogel in the study at hand, others—using different

histological processing methods—reported varying amounts of basophilic remnants of the poloxamer gel throughout the entire augmentation area after 14 weeks in a dog model[43] and even after 3 weeks postoperatively in a rabbit model.[44]

In the present study, similar values of rBSM, ST, and NB were found in both groups (PH, SPH), suggesting an equal biological behavior regarding degradation and bone remodeling rate. These findings are supported by animal experiments in dogs[43] and in rabbits,[19] using a pure P407 hydrogel in combination with hydroxyapatite (100% HA, HA/b-TCP 20/80, HA/b-TCP 40/60 and HA/b-TCP 15/85), showing no negative effect of P407 regarding bone remodeling.

Rheological measurements showed a temperature-based shift in viscosity and shear rates in P407 hydrogels. Other researchers support the correlation between increasing temperature and viscosity in P407 hydrogels.[15,45] Viscosity is also affected by increased poloxamer concentration or by adding molecules like hydroxypropyl beta-cyclodextrin.[14] The present study shows that the admixture of SiO_2 particles to P407 hydrogels (3 wt % SiO_2, 25 wt % P407, and 72 wt % water) also increases the viscosity. These findings support the theoretical model of changing material characteristics of poly(ethylene oxide)–poly(propylene oxide)–poly(ethylene oxide) block copolymer by adsorbing silica.[28] Combining a hydroxyapatite BSM with the modified hydrogel (3 wt % SiO_2, 25 wt % P407, and 72 wt % water) also affects the solubility in SBF. Since this study aimed to compare rheological similar BSM composites, PH30 and SPH25 were chosen for further solubility and in vivo analyses. Here, a lower solubility of SPH25 was observed which could either be attributed to the SiO_2 content or the lower hydrogel proportion.

Nevertheless, the observed lower solubility suggests a higher structural consistency of the BSM. It should be noted that such in vitro experiments only determine a static approach and can only represent the multidimensional effects in vivo to a limited extent. Because of the different amounts of liquid in the defect, the surface interaction areas, and the biological variability of individual biological systems, the in vitro and in vivo experiments are not comparable. However, following the idea of BSMs serving as a stable scaffold for bone healing, the higher structural consistency obtained by SiO_2-enrichment might be advantageous in more advanced bone defects.[43] Because of the simple bone defect in the in vivo experiment, further trials with more demanding bone defects (lacking three-dimensional stability) are needed to support the clinical benefit of higher structural consistency.

There has been growing interest in an injectable gel-forming polymeric hydrogel system for tissue engineering, which is desirable due to its minimally invasive delivery and reduced surgical risks. The ideal injectable polymer scaffold would be pliable at room temperature to allow incorporation of substances and cells for tissue engineering, facilitate minimally invasive application with good stability after implantation, be nontoxic, and be capable of interacting with the host tissue and biological environment.[45] Combining synthetic non-sintered low crystalline hydroxyapatite BSM with SiO_2-enriched P407 hydrogels improves the mechanical properties of the BSM and shows no negative effects on degradation or bone remodeling. Furthermore, the mix might enhance the handling properties. Future studies may focus on the hydrogel as a carrier for substances in tissue engineering, which could further enhance the biological response. Here, it has been shown that the release behavior of drug molecules from the hydrogel can be controlled by the hydrogel's composition and the drug ionic properties.[45] Future directions may focus on adding stem cells,[46] bioactive molecules like BMP,[47,48] or bioactive ions to enhance bone regeneration further.

5 | CONCLUSION

Based on the increased viscosity and the lower solubility of the SiO_2 hydrogel (SPH25), as well as the similar in vivo healing properties of PH30 and SPH25, adding SiO_2 to a P407 hydrogel-based hydroxyapatite BSM improves its mechanical stability. Additionally, the SiO_2-enrichment allows a reduction of the poloxamer proportion in the hydrogel simultaneously without impairing the material properties.

AUTHOR CONTRIBUTIONS

M.D., B.F., and T.G. carried out the conception and design of the presented experiments. M,D. and C.G. organized and supervised animal experiments, measurements, and data collection. M.D. did the animal experiments. F.Z. did the measurements of the histopathologic specimens, the rheological tests, and the solubility tests. M.D., D.H., P.W.K., C.G., and F.Z. analyzed the data, did the statistics, and drafted the manuscript. M.D., D.H., P.W.K., B.F., F.Z., C.G., and T.G. conducted the interpretation of the data.

ACKNOWLEDGMENTS

We thank Daniel Wolter for his excellent technical assistance.

FUNDING INFORMATION

This research received no specific grant from any funding agency in the public, commercial, or not-for-profit sectors.

CONFLICT OF INTEREST STATEMENT

GT is a member of the executive committee of Artoss GmbH, Rostock, Germany, and has been part of the group that developed NanoBone® S39.The other authors declare that they have no conflict of interest or financial interests related to any products involved in this study.

DATA AVAILABILITY STATEMENT

The datasets generated during and/or analyzed used in this manuscript are available from the corresponding author on reasonable request.

ORCID

Diana Heimes https://orcid.org/0000-0001-9899-7715
Michael Dau https://orcid.org/0000-0002-2619-3256

REFERENCES

1. Tang CL, Mahoney JL, McKee MD, et al. Donor site morbidity following vascularized fibular grafting. *Microsurgery*. 1998;18(6):383-386.
2. Dimitriou R, Mataliotakis GI, Angoules AG, Kanakaris NK, Giannoudis PV. Complications following autologous bone graft harvesting from the iliac crest and using the RIA: a systematic review. *Injury*. 2011;42(Suppl 2):S3-S15.
3. Heimes D, Pabst A, Becker P, et al. Comparison of morbidity-related parameters between autologous and allogeneic bone grafts for alveolar ridge augmentation from patients' perspective-a questionnaire-based cohort study. *Clin Implant Dent Relat Res*. 2023;26:170-182.
4. Finkemeier CG. Bone-grafting and bone-graft substitutes. *J Bone Joint Surg Am*. 2002;84(3):454-464.
5. Hettwer W. Synthetic bone replacement: current developments and perspectives. *Orthopade*. 2017;46(8):688-700.
6. Campion CR, Chander C, Buckland T, Hing K. Increasing strut porosity in silicate-substituted calcium-phosphate bone graft substitutes enhances osteogenesis. *J Biomed Mater Res B Appl Biomater*. 2011;97(2):245-254.
7. Majidinia M, Sadeghpour A, Yousefi B. The roles of signaling pathways in bone repair and regeneration. *J Cell Physiol*. 2018;233(4):2937-2948.
8. Al-Khateeb R, Olszewska-Czyz I. Biological molecules in dental applications: hyaluronic acid as a companion biomaterial for diverse dental applications. *Heliyon*. 2020;6(4):e03722.
9. D'Albis G, D'Albis V, Palma M, Plantamura M, Nizar A. Use of hyaluronic acid for regeneration of maxillofacial bones. *Genesis*. 2022;60(8–9):e23497.
10. Kyyak S, Pabst A, Heimes D, Kämmerer PW. The influence of hyaluronic acid biofunctionalization of a bovine bone substitute on osteoblast activity in vitro. *Materials (Basel)*. 2021;14(11):2885.
11. Kang H-J, Park SS, Saleh T, Ahn KM, Lee BT. In vitro and in vivo evaluation of Ca/P-hyaluronic acid/gelatin based novel dental plugs for one-step socket preservation. *Materials and Design*. 2020;194:108891.
12. Alcantara CEP, Castro MAA, de Noronha MS, et al. Hyaluronic acid accelerates bone repair in human dental sockets: a randomized triple-blind clinical trial. *Braz Oral Res*. 2018;32:e84.
13. Lorenz J, Barbeck M, Kirkpatrick C, Sader R, Lerner H, Ghanaati S. Injectable bone substitute material on the basis of beta-TCP and hyaluronan achieves complete bone regeneration while undergoing nearly complete degradation. *Int J Oral Maxillofac Implants*. 2018;33(3):636-644.
14. Bonacucina G, Spina M, Misici-Falzi M, et al. Effect of hydroxypropyl beta-cyclodextrin on the self-assembling and thermogelation properties of poloxamer 407. *Eur J Pharm Sci*. 2007;32(2):115-122.
15. Cho C-W, Shin S-C, Oh I-J. Thermorheologic properties of aqueous solutions and gels of poloxamer 407. *Drug Dev Ind Pharm*. 1997;23(12):1227-1232.
16. Veyries ML, Couarraze G, Geiger S, et al. Controlled release of vancomycin from poloxamer 407 gels. *Int J Pharm*. 1999;192(2):183-193.
17. Schmolka IR. Artificial skin. I. Preparation and properties of pluronic F-127 gels for treatment of burns. *J Biomed Mater Res*. 1972;6(6):571-582.
18. Park H, Park K. Biocompatibility issues of implantable drug delivery systems. *Pharm Res*. 1996;13(12):1770-1776.
19. Zhou AJ, Clokie CM, Peel SA. Bone formation in algae-derived and synthetic calcium phosphates with or without poloxamer. *J Craniofac Surg*. 2013;24(2):354-359.
20. Li C, Yan T, Lou Z, et al. Characterization and in vitro assessment of three-dimensional extrusion Mg-Sr codoped SiO(2)-complexed porous microhydroxyapatite whisker scaffolds for biomedical engineering. *Biomed Eng Online*. 2021;20(1):116.
21. Carlisle EM. Silicon as an essential trace element in animal nutrition. *Ciba Found Symp*. 1986;121:123-139.
22. Carlisle EM. Silicon: a possible factor in bone calcification. *Science*. 1970;167(3916):279-280.
23. Carlisle EM. Silicon: a requirement in bone formation independent of vitamin D1. *Calcif Tissue Int*. 1981;33(1):27-34.
24. Gotz W, Tobiasch E, Witzleben S, Schulze M. Effects of silicon compounds on biomineralization, osteogenesis, and hard tissue formation. *Pharmaceutics*. 2019;11(3):117.
25. Venkatraman SK, Swamiappan S. Review on calcium- and magnesium-based silicates for bone tissue engineering applications. *J Biomed Mater Res A*. 2020;108(7):1546-1562.
26. Dau M, Ganz C, Zaage F, Frerich B, Gerber T. Hydrogel-embedded nanocrystalline hydroxyapatite granules (elastic blocks) based on a cross-linked polyvinylpyrrolidone as bone grafting substitute in a rat tibia model. *Int J Nanomedicine*. 2017;12:1-12.
27. Dau M, Kämmerer PW, Henkel KO, Gerber T, Frerich B, Gundlach KKH. Bone formation in mono cortical mandibular critical size defects after augmentation with two synthetic nanostructured and one xenogenous hydroxyapatite bone substitute—in vivo animal study. *Clin Oral Implants Res*. 2016;27(5):597-603.
28. Sarkar B, Venugopal V, Tsianou M, Alexandridis P. Adsorption of Pluronic block copolymers on silica nanoparticles. *Colloids Surf A Physicochem Eng Asp*. 2013;422:155-164.
29. Sarkar B, Venugopal V, Bodratti AM, Tsianou M, Alexandridis P. Nanoparticle surface modification by amphiphilic polymers in aqueous media: role of polar organic solvents. *J Colloid Interface Sci*. 2013;397:1-8.
30. Gerber T, Lenz S, Holzhüter G, et al. Nanostructured bone grafting substitutes—a pathway to Osteoinductivity. *Key Engineering Materials*. 2011;493–494:147-162.
31. Gerike W, Bienengräber V, Henkel KO, et al. The manufacture of synthetic non-sintered and degradable bone grafting substitutes. *Folia Morphol*. 2006;65(1):54-55.
32. Gerber T, Holzhüter G, Götz W, Bienengräber V, Henkel KO, Rumpel E. Nanostructuring of biomaterials—a pathway to bone grafting substitute. *Eur J Trauma*. 2006;32:132-140.
33. Kilkenny C, Browne WJ, Cuthill IC, Emerson M, Altman DG. Improving bioscience research reporting: the ARRIVE guidelines for reporting animal research. *J Pharmacol Pharmacother*. 2010;1(2):94-99.
34. Dau M, Ganz C, Zaage F, et al. In vivo comparison of a granular and putty form of a sintered and a non-sintered silica-enhanced hydroxyapatite bone substitute material. *J Biomater Appl*. 2020;34(6):864-874.
35. Chang BS, Lee CK, Hong KS, et al. Osteoconduction at porous hydroxyapatite with various pore configurations. *Biomaterials*. 2000;21(12):1291-1298.
36. Habibovic P, Yuan H, van der Valk CM, Meijer G, van Blitterswijk CA, de Groot K. 3D microenvironment as essential element for osteoinduction by biomaterials. *Biomaterials*. 2005;26(17):3565-3575.
37. Klein M, Goetz H, Pazen S, al-Nawas B, Wagner W, Duschner H. Pore characteristics of bone substitute materials assessed by microcomputed tomography. *Clin Oral Implants Res*. 2009;20(1):67-74.
38. Klein MO, Kämmerer PW, Scholz T, Moergel M, Kirchmaier CM, al-Nawas B. Modulation of platelet activation and initial cytokine release by alloplastic bone substitute materials. *Clin Oral Implants Res*. 2010;21(3):336-345.
39. Lee S, Li Z, Meng D, et al. Effect of silicon-doped calcium phosphate cement on angiogenesis based on controlled macrophage polarization. *Acta Biochim Biophys Sin (Shanghai)*. 2021;53(11):1516-1526.
40. Alvarez Echazu M, Renou S, Alvarez G, Desimone M, Olmedo D. A collagen-silica-based biocomposite for potential application in bone tissue engineering. *J Biomed Mater Res A*. 2022;110(2):331-340.
41. Botelho CM, Brooks RA, Best SM, et al. Human osteoblast response to silicon-substituted hydroxyapatite. *J Biomed Mater Res A*. 2006;79(3):723-730.

42. Zhou AJ, Peel SA, Clokie CM. An evaluation of hydroxyapatite and biphasic calcium phosphate in combination with Pluronic F127 and BMP on bone repair. *J Craniofac Surg*. 2007;18(6):1264-1275.
43. Schliephake H, Drewes M, Mihatovic I, Schwarz F, Becker J, Iglhaut G. Use of a self-curing resorbable polymer in vertical ridge augmentations—a pilot study in dogs. *Clin Oral Implants Res*. 2014;25(4):435-440.
44. Miramond T, Aguado E, Goyenvalle E, Borget P, Baroth S, Daculsi G. In vivo comparative study of two injectable/moldable CalciumPhosphate bioceramics. *Key Eng Mater*. 2013;529:291-295.
45. Huh HW, Zhao L, Kim SY. Biomineralized biomimetic organic/inorganic hybrid hydrogels based on hyaluronic acid and poloxamer. *Carbohydr Polym*. 2015;126:130-140.
46. Beger B, Blatt S, Pabst AM, et al. Biofunctionalization of synthetic bone substitutes with angiogenic stem cells: influence on regeneration of critical-size bone defects in an in vivo murine model. *J Craniomaxillofac Surg*. 2018;46(9):1601-1608.
47. Cao SS, Li SY, Geng YM, et al. Prefabricated 3D-printed tissue-engineered bone for mandibular reconstruction: a preclinical translational study in primate. *ACS Biomater Sci Eng*. 2021;7(12):5727-5738.
48. Nokhbatolfoghahaei H, Bastami F, Farzad-Mohajeri S, et al. Prefabrication technique by preserving a muscular pedicle from masseter muscle as an in vivo bioreactor for reconstruction of mandibular critical-sized bone defects in canine models. *J Biomed Mater Res B Appl Biomater*. 2022;110(7):1675-1686.

How to cite this article: Kämmerer PW, Heimes D, Zaage F, et al. Improving material properties of a poloxamer P407 hydrogel-based hydroxyapatite bone substitute material by adding silica—A comparative in vivo study. *J Biomed Mater Res*. 2024;112(5):e35405. doi:10.1002/jbm.b.35405